ACS OMEGA

http://pubs.acs.org/journal/acsodf

Article

Neglected Importance of Anharmonicity in Quantifying the Renner−Teller Effect

Qing Lu*

Cite This: *ACS Omega* 2022, 7, 44078−44084

Read Online

ACCESS | Metrics & More | Article Recommendations | Supporting Information

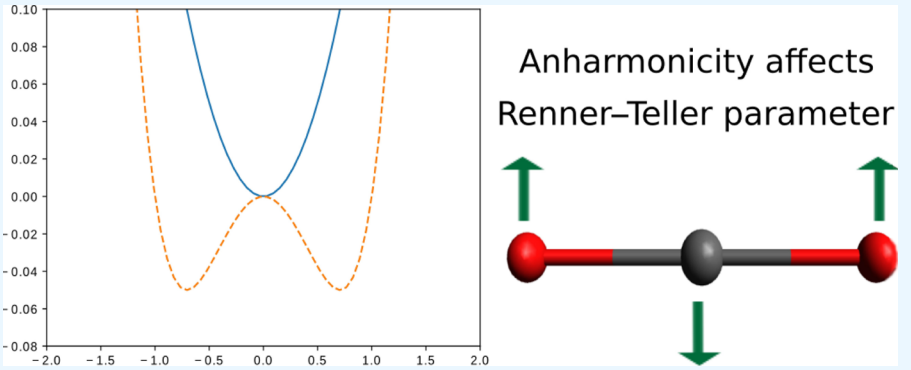

ABSTRACT: Linear molecules in degenerate electronic states are influenced by the Renner−Teller (RT) effect. Currently the formula to quantify this vibronic interaction only considers the harmonic term. However, such a harmonic formula cannot well describe molecules that have double-well potential along the bending coordinate. In this work, we propose a new formula to quantify the RT effect by explicitly including the anharmonic term. A sign function and a delta function are additionally included to distinguish different scenarios. It is mathematically proved that the new formula is capable of differentiating different degrees of RT splitting. Representative molecules of different types are calculated. According to the new formula, molecules experiencing a weak RT effect have a positive parameter smaller than 1. For those experiencing a medium RT effect, the parameter will be negative. For others experiencing a large RT effect, the parameter will be larger than 1.

INTRODUCTION

The Renner−Teller (RT) effect describes the energy splitting of degenerate states for linear molecules during bending motion.[1] It influences chemical behaviors of linear molecules in many aspects. In the field of direct laser cooling of polyatomic molecules, quite a few studied molecules possess a linear configuration during photon excitations.[2] For a molecule to be laser-coolable, it should stay at its ground vibronic state, which requires that it should have its vibrational branching ratio close to one.[3] If the molecule happens to be linear in the degenerate state, the RT effect influences the vibrational branching ratios, which then dictates the efficiencies of optical transition cycles. These imply that the linear laser-coolable molecules should experience a weak RT effect and thus preferably remain linear at relevant electronic states.[4] In addition to its significance in ultracold chemistry, the RT effect is important in the interpretation of complicated spectra.[5−7] The most famous example might be the spectral interpretation of the NH_2 radical.[8,9] By taking account of the RT effect, Pople and co-workers obtained a very good agreement between observed frequencies and calculated frequencies of the NH_2 radical. This in turn confirms Dressler and Ramsay's attributing of the absorption spectrum to transitions between two real components of the Π state (Figure 1c). Other illustrations, where the RT effect plays an important role, include enhancement of magnetism of luminescence properties by suppressing RT vibronic coupling or restriction of RT distortion,[10] bond stretch isomerism,[11] chemistry involving continuum processes,[12] or anomaly dynamic behaviors.[13]

Intuitively, different molecules would exhibit different behaviors when experiencing the RT distortion. As shown in Herzberg's famous book[14] as well as other's work,[9,15] the RT splitting can be classified into different types, although their criteria for categorization are not exactly the same. In our view, the RT splitting can be categorized into three types (Figure 1). The first type has both curves in a parabola form; the second type has the upper curve in a parabola form while the lower curve is in a double-well form; and the third type has both curves in a

Received: August 25, 2022
Accepted: November 10, 2022
Published: November 18, 2022

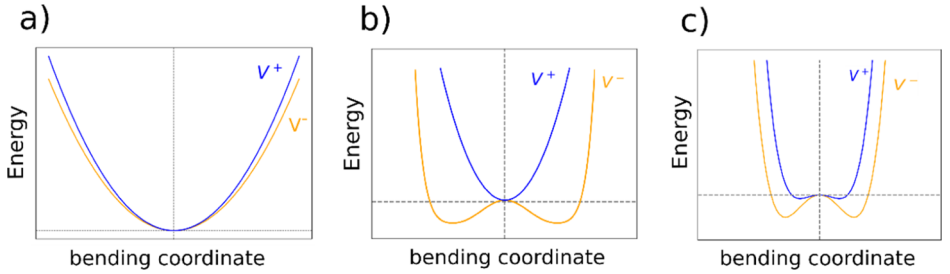

Figure 1. Different types of RT adiabatic potential energy curves along the bending coordinate. (a) both potential energy curves of a parabola shape; (b) upper potential energy curve of a parabola shape and lower potential energy curve of a double-well shape; (c) both potential energy curves of a double-well shape.

double-well form. The other categorizations have finer criteria such as the order of symmetries for the upper and lower curves or the curvature of the curves.

To describe the RT splitting, the RT parameter ε is introduced, so the upper (V^+) and lower (V^-) component curves are connected by ε

$$V^{\pm} = V_m(1 \pm \varepsilon) \tag{1}$$

where V_m is the mean potential or the zeroth-order potential. The upper and lower components are of different spatial symmetries, and different molecules may have different symmetries for the upper or lower components. Taking the CCP radical as an example, the upper and lower states are A′ and A″, respectively. However, for other molecules, the state symmetries might be the opposite. The RT parameter ε is defined as[16]

$$\varepsilon = \frac{V^+ - V^-}{V^+ + V^-} \tag{2}$$

As the molecule is symmetric with respect to the molecular axis, the bending potential must be an even function along the bending coordinate (q), so that

$$V_m(q) = \frac{1}{2}(V^+(q) + V^-(q)) = aq^2 + bq^4 + \ldots \tag{3}$$

$$V^+(q) - V^-(q) = \alpha q^2 + \beta q^4 + \ldots \tag{4}$$

where a and α are quadratic coefficients, while b and β are quartic coefficients. They, respectively, represent the force constant and the anharmonic correction. As the anharmonic terms are usually much smaller than the harmonic terms, the higher-order terms are usually neglected.[14,15] Therefore, the RT parameter ε becomes

$$\varepsilon = \frac{\alpha}{2a} = \frac{(\omega^+)^2 - (\omega^-)^2}{(\omega^+)^2 + (\omega^-)^2} \tag{5}$$

where ω^+ and ω^- are, respectively, the harmonic frequencies associated with the V^+ and V^- potentials.

This definition of ε has been widely used in characterizing the RT effect, even till today.[6,17−19] For an extension, very recently, it was shown that the NO molecule encapsulated in a fullerene can also experience a vibronic coupling effect very similar to the RT effect regarding the NO translation.[20] Thus, the RT parameter may not only characterize the distortion of linear molecules but also quantify energy splitting of more complex systems.

However, there is a flaw in the harmonic formula to quantify the RT effect. If only harmonic terms are used, combining eqs 3 and 4, the lower component of the potential energy curve (V^-) would be

$$V^- = \frac{1}{2}(2a - \alpha)q^2 \tag{6}$$

It is obvious that V^- is simply a parabola equation, which has one and only one minimum. Consequently, the double-well potential energy curve shown in Figure 1c can never be achieved. Therefore, one cannot compare the RT parameter ε_1 for the case corresponding to Figure 1a and the RT parameter ε_2 for the case corresponding to Figure 1c since the RT parameter ε cannot transit from case (a) to case (c). A consequence of this incapability is that the trend for molecular properties is not well recognized. For instance, in recent years, it has received significant attention for exploring polyatomic candidates suitable for direct laser cooling.[3,21] Our recent efforts try to understand why certain linear molecules are good laser-coolable candidates while others are not and try to setup a trend to make predictions. This leads us to compare the RT parameters. Nevertheless, as discussed, the harmonic RT parameter cannot characterize the double-well potential; therefore, the trend based on it cannot reflect the true physics.

Therefore, in this work, we propose a new formula to calculate the RT parameter ε_a. The subscript "a" stands for the inclusion of "anharmonic" terms into the formula to differentiate itself from the conventional RT parameter ε. This proposed parameter ε_a can well distinguish the three types of molecules. To examine the performance of the new formula, three types of molecules are studied. They include $^2\Pi$ CCN, $^2\Pi$ CCP, $^2\Pi$ HCSi, $^2\Pi$ OCS^+, and $^2\Pi$ NCO (type a), $^2A_1$ BH_2, $^2A_1$ AlH_2, $^2A_1$ SNO, and $^2A_1$ NO_2, (type b), and $^1A_1$ CH_2, $^1A_1$ SiH_2, $^1A_1$ GeH_2, and $^2B_1$ NH_2 (type c). As will be shown later, the new-defined parameter can well describe molecules for all types and shows a transition between different scenarios, which remedies the deficiency of the previous definition of the RT parameter.

METHODS

In this work, the CCN, CCP, HCSi, OCS^+, and NCO (type a), BH_2, AlH_2, SNO, and NO_2, (type b), and singlet CH_2, singlet SiH_2, singlet GeH_2, and NH_2 (type c) were calculated for their RT parameters ε_a. Unless explicitly stated, such as in cases of singlet CH_2, SiH_2, and GeH_2, all molecules are studied for their lowest spin state. Since the molecules have different term symbols for linear and bent configurations, symbols for the orbital angular momentum part of the term are not listed to avoid any confusion.

The local potential energy surfaces (PESs) were established for these molecules around their ground equilibrium geometry. The sampling of grid points and the fitting of PESs have been

https://doi.org/10.1021/acsomega.2c05494
ACS Omega 2022, 7, 44078−44084

described in previous studies.[7,22] For a brief summary, the range for the bond length spans from R_e-0.3 to R_e +0.5 in the unit of Bohr, where R_e is chosen close to the experimental value. The range for the bond angle spans from 180 to 100°. The PESs were obtained by the non-linear least-square fitting to the fifth-order polynomial in the displacement coordinates. The geometry minimum is obtained using the differential evolution algorithm.[23] The fitting was carried out using an in-house Python-based script.

For each grid point, the electronic energies were calculated by the state-averaged multi-reference configuration interaction method with the Davidson correction.[24] The C_s symmetry was used during the calculation. The full valence active space was used together with the cc-pVQZ basis sets.[25]

After obtaining the PES, the upper and lower bending curves are directly fitted to the second or fourth even order polynomial in the unit of radian with bond lengths equal to the equilibrium values

$$V_2 = aq^2 + C$$

$$V_4 = aq^2 + bq^4 + C \tag{7}$$

Neglecting the constant term, each bending energy curve can be described using the second- and fourth-order coefficients as the features of the potential energy curves. The feature length can be defined as

$$|V| = \sqrt{a^2 + b^2} \tag{8}$$

The RT parameter in eq 2 then becomes

$$\varepsilon = \frac{|V_+| - |V_-|}{|V_+| + |V_-|} \tag{9}$$

Notably, when the fourth-order coefficients are neglected, eq 9 reduces to eq 2.

Having extended the canonical definition of the RT parameter formula, the bending potential is fitted according to eq 7 to obtain the quadratic (a^+, a^-) and quartic (b^+, b^-) coefficients for upper and lower states. For the harmonic curve, the quartic coefficient is set to 0 and the second even order polynomial is used for fitting.

To distinguish different types of molecules, a sign function of $\frac{a^+}{a^-}$ is first introduced, where the $\text{sign}\left(\frac{a^+}{a^-}\right)$ returns 1 if the ratio of $\frac{a^+}{a^-}$ is positive, otherwise −1. Additionally, a delta function is introduced to exhibit the quartic effect. Eventually, the proposed RT parameter equation reads as

$$\varepsilon_a = \text{sign}\left(\frac{a^+}{a^-}\right)\left[\frac{|\sqrt{a_+^2 + b_+^2} - \sqrt{a_-^2 + b_-^2}|}{\sqrt{a_+^2 + b_+^2} + \sqrt{a_-^2 + b_-^2}} + (1 - \delta_{b_+,0})(1 - \delta_{b_-,0})\right] \tag{10}$$

The physical interpretations and applications of eq 10 are illustrated in detail in the next section.

RESULTS AND DISCUSSION

As discussed above, the harmonic RT parameter cannot characterize the double-well of potential V^-. Therefore, the anharmonic terms need to be included. Two features can be summarized for ε_a calculated using eq 10. First, the coefficients a and b for double-well curve fitting must possess different signs. Otherwise, the bending potential will be monotonical along the bending coordinate when the molecular configuration deviates from linearity. Moreover, the sign of a must be negative in order to have a downward parabola when the bending angle is small. As a result, the quadratic coefficients $a_\pm$ for type (a) molecules will both be positive; the coefficient, a_+ and a_- for type (b) molecules will be, respectively, positive and negative; and the coefficients $a_\pm$ for type (c) molecules will both be negative. Benefiting from this property, a sign function is included in the ε_a formula so that only type (b) molecules will have a negative RT parameter.

Second, if no quartic term is present in the bending expansion, the delta function in eq 10 will be 0. This corresponds to the type (a) situation. As discussed above, the sign function for type (a) molecules returns 1. Therefore, the proposed RT formula becomes similar to the canonical formula. The difference is that the canonical ε equation is based on the harmonic frequencies, while the proposed formula depends on the fitted quadratic coefficient, which is equivalent to the force constant. On a related note, having determined the sign function and the delta functions, the remaining part of eq 10 is a pure fractional number, namely, smaller than 1. On the other hand, when the quartic term is present, as for type (c) molecules, the delta functions remain in the bracket, and the final RT parameter will be greater than 1.

Overall, the RT parameter calculated using the proposed formula is robust to distinguish the three types of molecules, as is mathematically proved. In addition, the new formula only needs to fit a set of energies along the bending curve, which is computationally less expensive than the frequency calculations.

To illustrate the application of the new RT parameters, three types of molecules are studied. Figure 2 shows the bending curves of CCP, BH_2, and NH_2 molecules as examples for the three types of molecules. The bond lengths are kept fixed at the ground equilibrium values, which are obtained either from the National Institute of Standards and Technology computational chemistry comparison and benchmark database[26] or direct fitting of the local PES. The potential energy curves for other molecules and the corresponding bond lengths for fitting can be found in the Supporting Information.

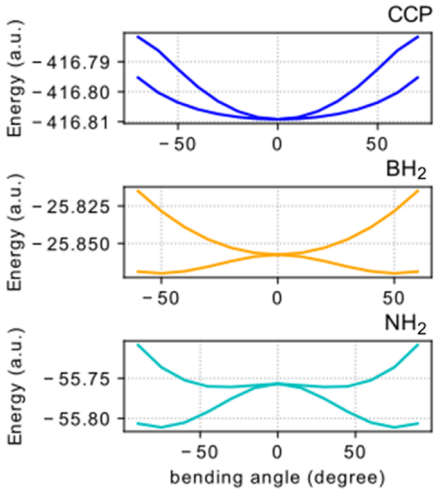

Figure 2. Different types of molecules defined in this work.

https://doi.org/10.1021/acsomega.2c05494
ACS Omega 2022, 7, 44078−44084

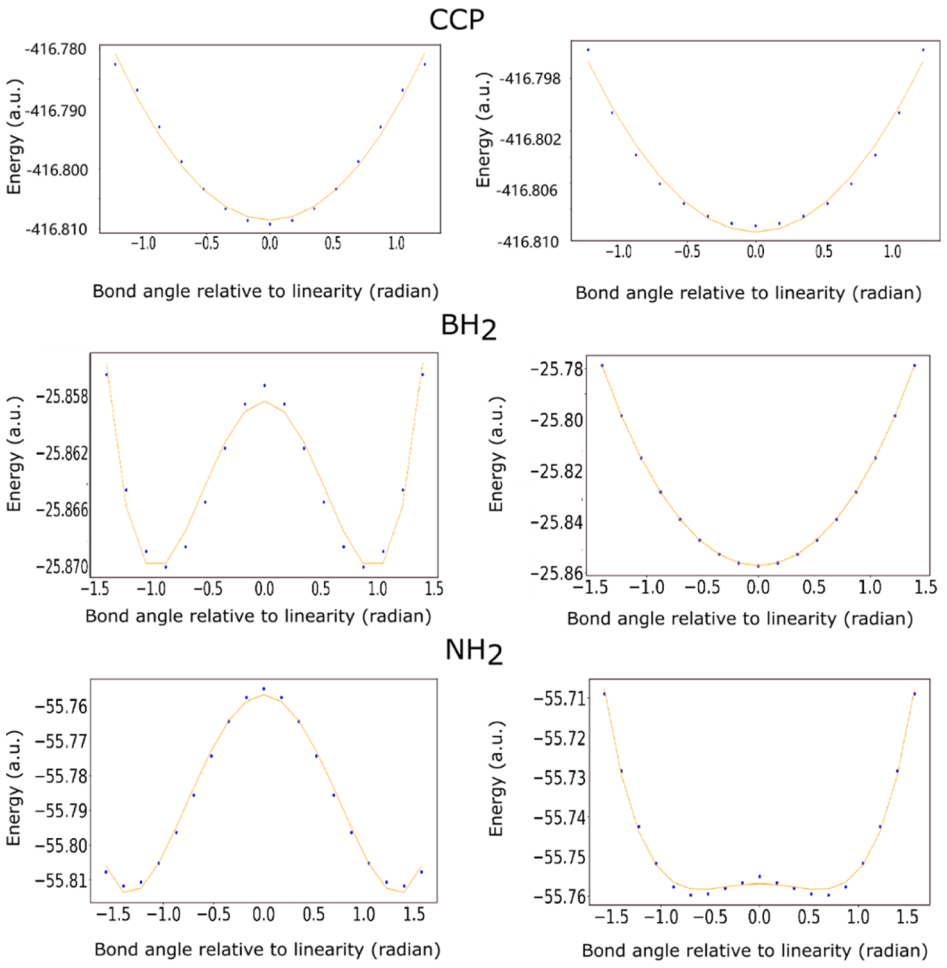

Figure 3. Fitting of lower (left) and upper (right) bending potential curves for the three types of molecules.

Figure 3 shows fitting of the upper and lower bending curves of CCP, BH_2, and NH_2. It becomes more evident that the bending curves follow the previous categorization. For type (a) molecules, as the RT parameter only depends on the quadratic terms.

$$\varepsilon_a = \frac{|a_+ - a_-|}{a_+ + a_-} \tag{11}$$

Assigning $t = \frac{a^+}{a^-}$ and taking advantage of the fact that V^+ is steeper than V^-, one will obtain that $a^+ > a^-$ and $t > 1$. The ε_a in eq 11 then becomes

$$\varepsilon_a = \frac{t - 1}{t + 1} \tag{12}$$

It can be easily shown that eq 12 increases monotonically with respect to t. Therefore, a larger RT parameter ε_a indicates a larger t, which in turn generally (but not always) indicates a larger splitting of the component curves. This remark is also valid for the RT parameter calculated using the canonical equation as eq 10 of ε_a for type (a) molecules is reduced to the canonical equation form.

For type (b) molecules, the RT parameters ε_a differentiate themselves from those of type (a) and type (c) molecules in term of the sign. To compare molecules within type (b), a similar analysis can be carried out. As the quartic coefficients are for higher-order terms, they are generally smaller in absolute values than the quadratic term. Thus, a larger absolute RT parameter suggests larger splitting, but caution should be given, and other characteristic parameters will become useful. For type (c) molecules, their RT parameters ε_a are greater than 1 and thus larger than those for type (a) molecules.

Table 1 shows the RT parameters calculated by both the proposed and canonical formulae for different types of molecules. It needs to be mentioned that the negative sign for the new-defined RT parameter ε_a has a different meaning from the canonical one. In the canonical case, the negative sign means that the A′ curve is lower in energy than the A” curve. In our framework, we do not distinguish whether the A′ curve is lower or higher in energy. Therefore, for type (a) molecules, the absolute values of canonical RT parameters are present for comparison. For type (b) and type (c) molecules, one or both of the component energy curves has a double-well shape; thus, the frequency is an imaginary number at the linear configuration. The RT parameters for these cases are consequently ill-defined.

Comparing the RT parameters for type (a) molecules, the two formulae generally have the same trend. The correlation coefficient reaches 0.96. The difference might result from the use of frequency or the “force constant”.

The new definition of the RT parameter is important in exploring laser-coolable molecules. For polyatomic molecules capable of being cooled to the ultracold regime, the excited state should retain nearly identical geometries to that of the ground state. One of the well-known laser-coolable molecules is the

https://doi.org/10.1021/acsomega.2c05494
ACS Omega 2022, 7, 44078−44084

Table 1. RT Parameter (ε_a) Calculated Using the Proposed Formula and the RT Parameter Calculated Using Canonical Formula

	type	ε_a(this work)	$\|\epsilon\|$[a]
CCN	a	0.35	0.43[b]
CCP	a	0.36	0.57[c]
HCSi	a	0.18	0.11[d]
OCS^+	a	0.15	0.10[e]
NCO	a	0.14	0.12−0.18[f]
BH_2	b	−0.22	
AlH_2	b	−0.16	
SNO	b	−0.26	
NO_2	b	−0.25	
NH_2	c	1.77	
CH_2	c	1.65	
SiH_2	c	1.42	
GeH_2	c	1.85	

[a]Absolute value of the RT parameter from canonical formula. [b]Adapted from ref 6. [c]Adapted from ref 7. [d]Adapted from ref 17. [e]Adapted from ref 18. [f]Adapted from ref 27.

alkaline-earth metal monohydroxide, such as the CaOH molecule.[4] The ground state of the CaOH molecule is the Σ state, while its first excited state is the Π state. The Σ state is a non-degenerate state, so it will not experience the RT splitting. On the contrary, the Π state is capable of RT splitting. As the geometry change needs to be minimal for being laser-coolable, the molecule needs to have a small RT parameter (ε_a) so that the linear configuration remains as the equilibrium. In fact, the CaOH molecule does have a parabola bending potential (Figure 4), and its ε_a is calculated to be 0.24.

A further conjecture can be made based on the current framework that the type (c) molecule also has the potential to be laser-coolable as long as the bond lengths and bond angles are similar between the upper and lower states. In fact, very recent studies[28] indeed propose that bent molecules such as SOH and CaSH can also be good laser-coolable molecules. The current work helps rationalize their hypothesis. On the contrary, if a molecule belongs to a type (b) molecule, then it would not be a good laser-coolable molecule, and it would feature a negative RT parameter. Lastly, it should be noted that the above analysis is a necessary but not sufficient condition to find laser-coolable molecules.

CONCLUSIONS

In this work, a new formula to quantify the RT effect is proposed by explicitly including the anharmonic term. The formula is capable of distinguishing three types of RT splitting with distinct RT parameters. For type (a) molecules, which experience a weak RT effect, they have a positive RT parameter smaller than 1. For type (b) molecules experiencing a medium RT effect, the RT parameter will be negative. For molecules experiencing a large RT effect, the RT parameter will be larger than 1. The proposed formula extends the conventional one and has a wider range of applications, such as helping rationalize recent laser-cooling studies and helping predict novel laser-coolable molecules.

ASSOCIATED CONTENT

Supporting Information

The Supporting Information is available free of charge at https://pubs.acs.org/doi/10.1021/acsomega.2c05494.

Bending potential energy curves for the studied molecules along with the corresponding bond length and the fitted quadratic and quartic coefficients for the studied molecules (PDF)

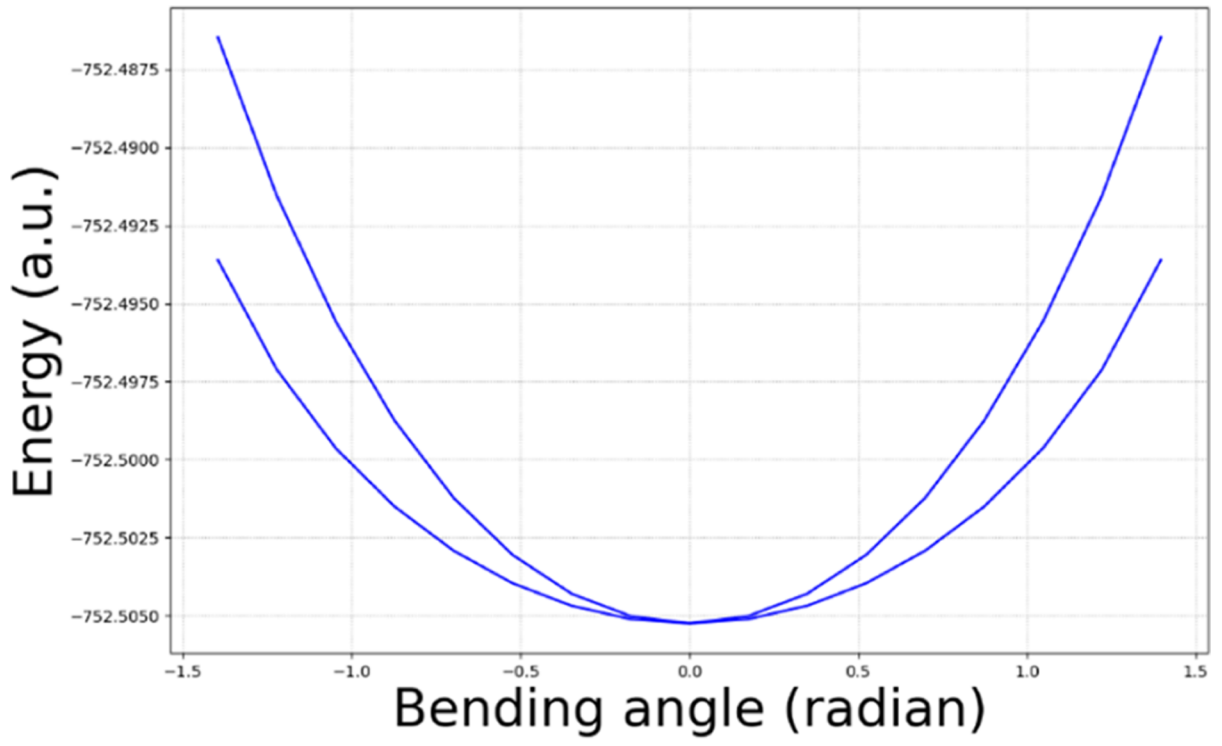

Figure 4. Bending potential curves of the $CaOH^2\Pi$ state.

https://doi.org/10.1021/acsomega.2c05494
ACS Omega 2022, 7, 44078−44084

AUTHOR INFORMATION

Corresponding Author

Qing Lu − *Beijing National Laboratory for Molecular Sciences, Institute of Chemistry, Chinese Academy of Sciences, Beijing 100190, China;* orcid.org/0000-0003-4063-9100; Email: qinglu@iccas.ac.cn

Complete contact information is available at: https://pubs.acs.org/10.1021/acsomega.2c05494

Notes

The author declares no competing financial interest.

ACKNOWLEDGMENTS

This work was supported by the Beijing Natural Science Foundation (no. 2214065) and National Natural Science Foundation of China (no. 22003068).

REFERENCES

(1) Jungen, C.; Merer, A. J. Orbital angular momentum in triatomic molecules. *Mol. Phys.* **1980**, *40*, 1−23.

(2) Baum, L.; Vilas, N. B.; Hallas, C.; Augenbraun, B. L.; Raval, S.; Mitra, D.; Doyle, J. M. Establishing a nearly closed cycling transition in a polyatomic molecule. *Phys. Rev. A* **2021**, *103*, 043111. (a) Owens, A.; Clark, V. H. J.; Mitrushchenkov, A.; Yurchenko, S. N.; Tennyson, J. Theoretical rovibronic spectroscopy of the calcium monohydroxide radical (CaOH). *J. Chem. Phys.* **2021**, *154*, 234302.

(3) Fitch, N. J.; Tarbutt, M. R.Laser-cooled molecules. In *Advances In Atomic, Molecular, and Optical Physics*; Dimauro, L. F., Perrin, H., Yelin, S. F., Eds.; Academic Press, 2021; Vol. *70*, Chapter 3, pp 157−262.

(4) Isaev, T. A. Direct laser cooling of molecules. *Phys. Usp.* **2020**, *63*, 289−302.

(5) Brünken, S.; Lipparini, F.; Stoffels, A.; Jusko, P.; Redlich, B.; Gauss, J.; Schlemmer, S. Gas-phase vibrational spectroscopy of the hydrocarbon cations l-C_3H^+, HC_3H^+, and c-$C_3H_2^+$: structures, isomers, and the influence of Ne-tagging. *J. Phys. Chem. A* **2019**, *123*, 8053−8062. (a) Lyle, J.; Jagau, T.-C.; Mabbs, R. Spectroscopy of temporary anion states: Renner−Teller coupling and electronic autodetachment in copper difluoride anion. *Faraday Discuss.* **2019**, *217*, 533−546. (b) Coudert, L. H.; Gans, B.; Garcia, G. A.; Loison, J.-C. Renner-Teller effects in the photoelectron spectra of CNC, CCN, and HCCN. *J. Chem. Phys.* **2018**, *148*, 054302. (c) Freund, J.; Kempf, S. C. G.; Jensen, P.; Nagashima, U.; Hirano, T. Computational spectroscopy of NCS in the Renner-degenerate electronic state X2Π. *J. Mol. Spectrosc.* **2018**, *345*, 31−38.

(6) Hill, J. G.; Mitrushchenkov, A.; Yousaf, K. E.; Peterson, K. A. Accurate ab initio ro-vibronic spectroscopy of the $X^2\Pi$ CCN radical using explicitly correlated methods. *J. Chem. Phys.* **2011**, *135*, 144309.

(7) Lu, Q. Accurate ab initio vibronic spectroscopy of the CCP and CCAs radicals. *Chem. Phys. Lett.* **2020**, *739*, 137017.

(8) Pople, J. A.; Longuet-Higgins, H. C. Theory of the Renner effect in the NH_2 radical. *Mol. Phys.* **1958**, *1*, 372−383.

(9) Dressler, K.; Ramsay, D. A. The electronic absorption spectra of NH_2 and ND_2. *Phil. Trans. Roy. Soc. Lond. Math. Phys. Sci.* **1959**, *251*, 553−602.

(10) Huzan, M. S.; Fix, M.; Aramini, M.; Bencok, P.; Mosselmans, J. F. W.; Hayama, S.; Breitner, F. A.; Gee, L. B.; Titus, C. J.; Arrio, M.-A.; et al. Single-ion magnetism in the extended solid-state: insights from X-ray absorption and emission spectroscopy. *Chem. Sci.* **2020**, *11*, 11801−11810. (a) Li, L.; Ravinson, D. S. M.; Haiges, R.; Djurovich, P. I.; Thompson, M. E. Enhancement of the luminescent efficiency in carbene-Au[I];-aryl complexes by the restriction of Renner−Teller distortion and bond rotation. *J. Am. Chem. Soc.* **2020**, *142*, 6158−6172.

(11) Homray, M.; Mondal, S.; Misra, A.; Chattaraj, P. K. Bond stretch isomerism in Be_3^{2-} driven by the Renner−Teller effect. *Phys. Chem. Chem. Phys.* **2019**, *21*, 7996−8003.

(12) Jungen, C. The Renner-Teller effect revisited 40 years later. *J. Mol. Spectrosc.* **2019**, *363*, 111172.

(13) Han, S.; Sun, G.; Zheng, X.; Song, Y.; Dawes, R.; Xie, D.; Zhang, J.; Guo, H. Rotational modulation of A^2A''-state photodissociation of HCO via Renner−Teller nonadiabatic transitions. *J. Phys. Chem. Lett.* **2021**, *12*, 6582−6588. (a) Gamallo, P.; González, M.; Petrongolo, C. Quantum Dynamics of Nonadiabatic Renner−Teller Effects in Atom + Diatom Collisions. *J. Phys. Chem. A* **2021**, *125*, 6637−6652.

(14) Herzberg, G.Molecular spectra and molecular structure. *Electronic spectra and electronic structure of polyatomic molecules*; Van Nostrand Reinhold, 1966; Vol. 3.

(15) Lee, T. J.; Fox, D. J.; Schaefer, H. F.; Pitzer, R. M. Analytic second derivatives for Renner−Teller potential energy surfaces. Examples of the five distinct cases. *J. Chem. Phys.* **1984**, *81*, 356−361.

(16) Renner, R. Zur Theorie der Wechselwirkung zwischen Elektronen- und Kernbewegung bei dreiatomigen, stabförmigen Molekülen. *Z. Phys.* **1934**, *92*, 172−193.

(17) Sari, L.; Gonzales, J. M.; Yamaguchi, Y.; Schaefer, H. F. The X $^2\Pi$ and $\tilde{A}$ $^2\Sigma^+$ electronic states of the HCSi radical: Characterization of the Renner−Teller effect in the ground state. *J. Chem. Phys.* **2001**, *114*, 4472−4478.

(18) Wheeler, S. E.; Simmonett, A. C.; Schaefer, H. F. Renner−Teller Bending Frequencies of the $\tilde{A}$ $^2\Pi$ State of OCS^+. *J. Phys. Chem. A* **2007**, *111*, 4551−4555.

(19) Finney, B.; Mitrushchenkov, A. O.; Francisco, J. S.; Peterson, K. A. Ab initio ro-vibronic spectroscopy of the Π^2 PCS radical and Σ^+ $^1PCS^-$ anion. *J. Chem. Phys.* **2016**, *145*, 224303. (a) Gharaibeh, M. A.; Clouthier, D. J. A laser-induced fluorescence study of the jet-cooled nitrous oxide cation (N2O+). *J. Chem. Phys.* **2012**, *136*, 044318. (b) Pernpointner, M.; Salopiata, F. A four-component quadratic vibronic coupling approach to the Renner−Teller effect in linear triatomic molecules. The 2Pi1/2 2Pi3/2 manifold of BrCN+and ClCN +. *J. Phys. B: At., Mol. Opt. Phys.* **2013**, *46*, 125101. (c) Tarroni, R.; Clouthier, D. J. Giant Renner−Teller vibronic coupling in the BF_2 radical: An ab initio study of the X A^{21} and A Π^2 electronic states. *J. Chem. Phys.* **2010**, *133*, 064304. (d) Wei, J.; Grimminger, R. A.; Sunahori, F. X.; Clouthier, D. J. Electronic spectroscopy of the jet-cooled arsenic dicarbide (C2As) free radical. *J. Chem. Phys.* **2008**, *129*, 134307.

(20) Hauser, A. W.; Pototschnig, J. V. Vibronic Coupling in Spherically Encapsulated, Diatomic Molecules: Prediction of a Renner−Teller-like Effect for Endofullerenes. *J. Phys. Chem. A* **2022**, *126*, 1674−1680.

(21) Tarbutt, M. R. Laser cooling of molecules. *Contemp. Phys.* **2018**, *59*, 356−376.

(22) Lu, Q.; Peterson, K. A. Coupled cluster spectroscopic properties of the coinage metal nitrosyls, M−NO (M = Cu, Ag, Au). *Theor. Chem. Acc.* **2020**, *139*, 81.

(23) Bilal; Pant, M.; Zaheer, H.; Garcia-Hernandez, L.; Abraham, A. Differential Evolution: A review of more than two decades of research. *Eng. Appl. Artif. Intell.* **2020**, *90*, 103479.

(24) Knowles, P. J.; Werner, H.-J. Internally contracted multi-configuration-reference configuration interaction calculations for excited states. *Theor. Chim. Acta* **1992**, *84*, 95−103. (a) Werner, H. J.; Knowles, P. J. An efficient internally contracted multiconfiguration−reference configuration interaction method. *J. Chem. Phys.* **1988**, *89*, 5803−5814.

(25) Dunning, T. H. Gaussian basis sets for use in correlated molecular calculations. I. The atoms boron through neon and hydrogen. *J. Chem. Phys.* **1989**, *90*, 1007−1023.

(26) Johnson, R. D., III*NIST Computational Chemistry Comparison and Benchmark Database*, 2022.

(27) Kashinski, D. O.; Radziewicz, T. J.; Suarez, M. G.; Stephens, C. C.; Byrd, E. F. C. Density functional theory calculation of the Renner−Teller effect in NCO: Preliminary assessment of exact exchange energy on the accuracy of the Renner coefficient. *Int. J. Quantum Chem.* **2021**, *121*, No. e26804.

(28) Liu, L.; Yang, C.-L.; Sun, Z.-P.; Wang, M.-S.; Ma, X.-G. Direct laser cooling schemes for the triatomic SOH and SeOH molecules

based on ab initio electronic properties. *Phys. Chem. Chem. Phys.* **2021**, *23*, 2392−2397. (a) Augenbraun, B. L.; Doyle, J. M.; Zelevinsky, T.; Kozyryev, I. Molecular asymmetry and optical cycling: laser cooling asymmetric top molecules. *Phys. Rev. X* **2020**, *10*, 031022.

https://doi.org/10.1021/acsomega.2c05494
ACS Omega 2022, 7, 44078−44084